applied optics

Shaping of cylindrical and 3D ellipsoidal beams for electron photoinjector laser drivers

S. Yu. Mironov,[1,*] A. K. Potemkin,[1] E. I. Gacheva,[1] A. V. Andrianov,[1] V. V. Zelenogorskii,[1] M. Krasilnikov,[2] F. Stephan,[2] and E. A. Khazanov[1]

[1]Federal Research Center Institute of Applied Physics of the Russian Academy of Sciences, 46 Uljanov Street, Nizhny Novgorod 603950, Russia
[2]Deutsches Elektronen-Synchrotron a Research Centre, Platanenallee 6, Zeuthen D-15738, Germany
*Corresponding author: Sergey. Mironov@mail.ru

Received 3 November 2015; revised 25 January 2016; accepted 28 January 2016; posted 29 January 2016 (Doc. ID 253273); published 26 February 2016

With the use of spatial light modulators it became possible to implement in experiments the method of controlling the space–time intensity distribution of femtosecond laser pulses stretched to picosecond duration. Cylindrical and quasi-ellipsoidal intensity distributions were obtained and characterized by means of a 2D spectrograph and a cross-correlator.

OCIS codes: (140.3300) Laser beam shaping; (140.3510) Lasers, fiber; (140.3295) Laser beam characterization; (070.6120) Spatial light modulators.

http://dx.doi.org/10.1364/AO.55.001630

1. INTRODUCTION

A present day photoinjector for high-power free-electron lasers must meet stringent requirements on peak brightness, duty factor, and stability of generated electron bunches. This demands generation of relatively short electron beams (10–100 ps) with sufficiently high charge (~1 nC), average kinetic energy of the order 5–7 MeV and small (<1 mm · mrad) normalized transverse emittance. Currently, works on generation of such electron bunches are under way in major accelerators worldwide. These include, in particular, Stanford Linear Accelerator (SLAC) in the USA, Deutsches Elektronen-Synchrotron (DESY) in Germany with branches in Hamburg (FLASH accelerator) and in Zeuthen (PITZ photoinjector test facility), as well as KEK in Japan and Joint Institute of Nuclear Research in Dubna, Russia.

Photoinjectors with laser drivers also referred to as photocathode lasers [1,2] are generally used in this research. By way of example we can mention two recent bright results. Electron bunches with a charge of 1 nC and emittance of 2.1 mm·mrad at the energy of 100 MeV were generated at the DESY photoinjector for the FLASH accelerator with the use of 10 ps Gaussian laser pulses [3]. Normalized emittance of ~0.7 mm · mrad [4] that is a record low for 1 nC electron bunches was obtained at the PITZ photoinjector using 21.5 ps trapezoidal laser pulses (quasi-cylindrical beams) with 2 ps fronts [5].

It is well known that control of intensity distribution of photocathode laser pulses is one of the key instruments for optimizing parameters of electron bunches [6]. For minimization of normalized transverse emittance, a 3D ellipsoidal charge distribution (Kapchinskij–Vladimirskij distribution) is demanded [7]. The first step toward producing electron bunches with extremely small emittance is to form laser beams with cylindrical and 3D ellipsoidal intensity distributions in space. In such laser beams the intensity must have constant value inside the cylinder or ellipsoid and be strictly equal to zero outside. It is important to note that such laser pulses cannot be generated in experiments because of infinite values of field derivative at the boundary. Hence, it is reasonable to consider the electric field of shaped laser pulses using an appropriate fuzzy function, super-Gaussian for instance, and call the corresponding distributions quasi-ellipsoidal and quasi-cylindrical.

In the present paper we will consider the scheme and operation of a 3D pulse shaper, as well as specific features of its optimal use for profiling optical pulses of a photocathode laser. Results of generating laser pulses with quasi-cylindrical and quasi-ellipsoidal intensity distributions obtained in the experiment will be presented.

2. OPERATION OF 3D SHAPER OF INTENSITY DISTRIBUTIONS

Ellipsoidal distribution may be considered as a beam with a diameter varying along the propagation coordinate or as a rectangular pulse of light with a duration changing at different points of the aperture. Two descriptions of the same 3D profiled intensity distribution correspond to two approaches of its formation. The authors of [8] used an acousto-optic modulator DAZZLER to shape quasi-ellipsoidal intensity distribution in the focus of a strongly aberrating lens, i.e., with the change of

the diameter along the longitudinal propagation coordinate. Here we adhere to the second approach, i.e., we shape a rectangular pulse with duration dependent on the transverse coordinate of the laser beam. The duration is maximal on beam axis and minimal at the aperture edge. For the region related to photoelectron emission and further acceleration of the electron beam, quasi-ellipsoidal distribution with a transverse size of about 1 mm and a longitudinal size of 3–9 mm is demanded, which corresponds to a pulse duration of 10–30 ps. Traditional modulators do not fit for such short time intervals. This problem can be solved by controlling spectral (amplitude and phase) characteristics of the initial pulses [9]. In the majority of cases, the amplitude and phase of the initial pulse spectrum are transformed by means of amplitude and phase masks placed inside an optical compressor with zero frequency dispersion. The schematic diagram of such a compressor is presented in Fig. 1.

Confocal lenses F1 and F2 form a Kepler telescope. To prevent additional frequency dispersion from the intensity distribution shaper, diffraction gratings are placed at a focal distance from the lenses for the telescope to transfer the image from one grating to the other. The mask $M(\omega)$ in the focal plane of the telescope allows controlling the amplitude and phase of the optical pulse spectrum, thereby providing the desired space–time intensity distribution. The scheme presented in Fig. 1 can be used to control space–time distribution of pulses with appreciable linear frequency modulation, also referred to as spectrons [10]. The spectral intensity distribution envelope of such pulses repeats the time envelope and the frequency is linearly proportional to time. If the Kepler telescope is formed by cylindrical lenses, then the spectral intensity distribution in the focal plane is two-dimensional. In this case, to control duration at different points of transversal intensity distribution it suffices to change the corresponding transmitted spectrum band. This scheme has two main drawbacks: (i) impossibility to shape axially symmetric space–time intensity distribution, and (ii) strong astigmatism induced by cylindrical Kepler telescope due to image transfer from diffraction grating in one plane only. The first drawback may be overcome using multiple passages of the beam through the 3D pulse shaper with a turn of the image by a certain angle. The second drawback may be eliminated almost completely by compensating astigmatism by means of a complementary cylindrical telescope turned by 90° with respect to the initial one.

Reflective spatial light modulators (SLMs) may be used as a mask $M(\omega)$. It is worth noting that modulators allow controlling the phase spectrum and in combination with a polarizer and a half-wave plate they can also be used to control the amplitude of the spectral components. We used Hamamatsu SLMs (LCOS-SLM X10468-03), which have both good reflectance and minimum induced noise.

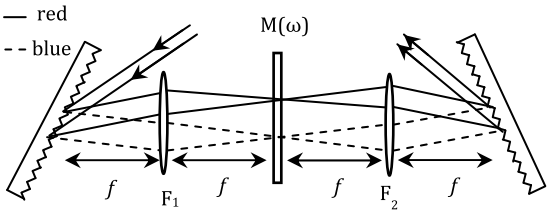

Fig. 1. Schematic diagram of 3D shaper of laser pulse intensity distribution.

3. THEORY OF SHAPING QUASI-CYLINDRICAL OPTICAL BEAMS

Let us consider a possibility of using an amplitude spectrum mask for shaping quasi-rectangular optical pulses. We assume that the initial pulse is a linear frequency-modulated pulse and its duration T greatly exceeds the duration of a spectrally limited pulse T_F. We assume for definiteness that the initial spectrum has Gaussian distribution and quadratic phase modulation (which corresponds to linear frequency modulation):

$$S(\Omega) = S_0 \cdot e^{-2\ln(2)\cdot\frac{\Omega^2}{\Delta\Omega^2} - i\frac{\alpha\cdot\Omega^2}{2}}. \tag{1}$$

Here, S_0 is spectrum amplitude, Ω is central frequency offset, and $\Delta\Omega = 4\ln(2)/T_F$ is FWHM spectral intensity. This distribution corresponds to the pulse in the time domain

$$A(t) = \int_{-\infty}^{\infty} S(\Omega)\cdot e^{i\cdot\Omega\cdot t}\mathrm{d}\Omega = \frac{\sqrt{2\pi}\cdot\Delta\Omega\cdot S_0}{\sqrt{4\cdot\ln(2) + i\cdot\alpha\cdot\Delta\Omega^2}}\cdot e^{-2\ln(2)\frac{t^2}{T^2} + i\frac{\alpha_t\cdot t^2}{2}}, \tag{2}$$

where $T = T_F\sqrt{1 + \frac{16\cdot\ln(2)^2\cdot\alpha^2}{T_F^4}}$, $\alpha_t = \frac{\alpha\cdot\Delta\Omega^2}{T_F^2 + \alpha^2\cdot\Delta\Omega^2}$.

One can see that Gaussian pulse shape corresponds to Gaussian spectrum distribution. If the condition $T \gg T_F$ is fulfilled and if there is linear frequency modulation, the time distribution repeats the intensity distribution in the spectral region [10]. Such pulses will be the subject of our interest in this paper.

Clearly, for shaping quasi-rectangular chirped pulses, quasi-rectangular spectrum distribution should be produced. Let us consider an ideal case of perfect rectangular spectrum distribution obtained from the initial Gaussian distribution. We can take for this purpose spectral mask of the form Eq. (3) used for the distribution $|S(\Omega)|^2$:

$$M_R(\Omega) = \begin{cases} \exp\left(4\cdot\ln(2)\frac{\Omega^2 - \Lambda^2}{\Delta\Omega^2}\right), & |\Omega| < \Lambda \\ 0, & |\Omega| > \Lambda \end{cases}. \tag{3}$$

The resulting spectrum will be a $2\cdot\Lambda$ wide rectangle. The energy efficiency of this mask is defined by

$$\eta = \sqrt{\frac{16\ln(2)}{\pi}}\cdot\frac{\Lambda}{\Delta\Omega}\cdot e^{-4\ln(2)\frac{\Lambda^2}{\Delta\Omega^2}}. \tag{4}$$

For $\Lambda \to 0$ and $\Lambda \to \infty$, $\eta \to 0$. The transmission is maximal $\eta_{\max} = \sqrt{\frac{2}{\pi\cdot e}} \sim 0.48$ for $\Lambda_{\max} = \frac{\Delta\Omega}{\sqrt{8\cdot\ln(2)}}$. Thus, making use of the spectrum amplitude mask Eq. (3) in an optimal case it is possible to obtain a rectangular spectrum with 48% efficiency.

In the considered approximation, a chirped optical pulse with rectangular spectrum will have quasi-rectangular intensity distribution in time. By transmitting this radiation through a round diaphragm it is possible to produce quasi-cylindrical beams analogous to the ones used in the works [4,5]. If the initial transverse intensity distribution is Gaussian, then N% decrease of intensity from the center to the edge of the diaphragm corresponds to the transmission of N% of the total

beam energy. Consequently, if a Gaussian beam with Gaussian spectrum is transmitted through the mask Eq. (3) having width $\Lambda = \Lambda_{max}$, and then through the diaphragm forming a 10% intensity drop from the center to the edge, then the total efficiency of shaping a 3D cylindrical beam will be 4.8%, which is very small indeed. The efficiency may be increased substantially using an apodizing diaphragm made of crystal quartz [11] or a π-shaper [12].

The spectral width $2 \cdot \Lambda_{max}$ is related to the duration of quasi-rectangular pulses T_r by $2 \cdot \Lambda_{max} = \alpha_t \cdot T_r$. Using this relation as well as formulas Eq. (2) and the condition $(T \gg T_F)$ we can readily show that the duration of the Gaussian pulse T to which a spectrally limited pulse must be stretched for producing a rectangular pulse having duration T_r with the best efficiency (from the energy viewpoint) may be found from the following expression:

$$T \approx \sqrt{2\ln(2)}\,T_r \approx 1.17 \cdot T_r. \tag{5}$$

A rectangular spectrum corresponds to modulated intensity distribution in time, even for pulses for which $(T \gg T_F)$. The impact of modulation may be reduced by means of a smoothed mask used for the amplitude of the spectrum $S_r(\Omega) = M_G(\Omega) \cdot S(\Omega)$,

$$M_G(\Omega) = \exp\left(-\left(\frac{\Omega}{\Lambda}\right)^{2N}\right) \cdot \begin{cases} \exp\left(2 \cdot \ln(2)\,\frac{\Omega^2-\Lambda^2}{\Delta\Omega^2}\right), & |\Omega| < \Lambda \\ 1, & |\Omega| > \Lambda \end{cases}, \tag{6}$$

where N is natural number. For the mask Eq. (6), the resulting spectrum amplitude has no jumps of derivative. Application of such a mask to the Gaussian spectrum of chirped pulses Eq. (1) permits shaping a quasi-rectangular temporal intensity distribution. An example will be given below when we will compare experimental and theoretical data.

An important parameter of the obtained profiled quasi-rectangular pulse is its front duration τ_F defined as the intensity rise time from the 0.1 to the 0.9 level of the maximum value. In application to laser drivers for photoinjectors, of specific interest are rectangular pulses with duration T_r in the 10–100 ps range. The pulse front τ_F as a function of duration T_r obtained in application to the considered optical pulses is plotted in Fig. 2(a) for different values of parameter N in the mask Eq. (6). We used for modeling the initial Gaussian pulse with a spectral width (FWHM) of 7.3 nm and a central wavelength

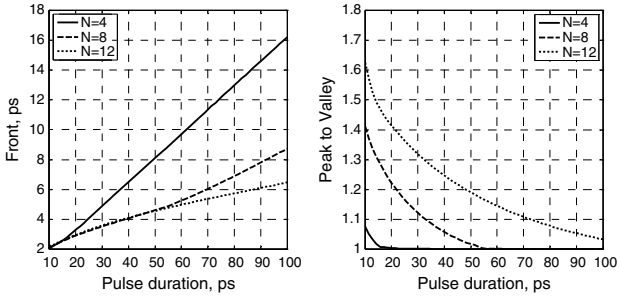

Fig. 2. (a) Pulse front τ_F and (b) parameter PV versus rectangular pulse duration T_r for $N = 4, 8, 12$.

of 1033 nm corresponding to our experimental parameters. Pulse stretching and spectrum cutting were optimal for each value of T_r. The pulse front increased with increasing duration of the rectangular pulse, which is a limitation of the method as pulses with sharp fronts cannot be produced. Front sharpness may be improved by increasing the power of N in the mask Eq. (6). This, however, is accompanied by an increase in the value of parameter PV (peak to valley) characterizing modulation in the region of the principal pulse (excluding slopes of the pulse) and defined as the maximum-to-minimum intensity ratio. The parameter PV as a function of rectangular pulse duration is plotted in Fig. 2(b) for $N = 4, 8, 12$. The efficiency of shaping quasi-rectangular pulses also depends on the power of N and is 42%, 45%, and 46%, respectively, for the values given above. When $N \to \infty$, the mask Eq. (6) transforms to Eq. (3) and, hence, the shaping efficiency tends to 48%. The power of N for experiment is determined by the initial pulse and requirements to the profiled pulse fronts and modulation. Note that to produce shorter fronts and to minimize the parameter PV, a phase mask is needed in addition to an amplitude mask.

The considered approach may be adapted for generating quasi-ellipsoidal pulses by setting a 2D (elliptical) amplitude mask in the 3D pulse shaper (Fig. 1), if cylindrical lenses are used in the Kepler telescope. Below we will present examples of using such a mask in the experiment.

4. DESCRIPTION OF THE EXPERIMENTAL SETUP

The optical scheme of the setup used in the experiments is presented in Fig. 3. An Yb fiber laser with two channels (operating and diagnostic) at the output is used as a source of optical pulses. Radiation from the operating channel is transmitted to the 3D pulse shaper for obtaining quasi-cylindrical or quasi-ellipsoidal beams. Radiation from the diagnostic channel is compressed to minimal duration (~250 fs) and is forwarded

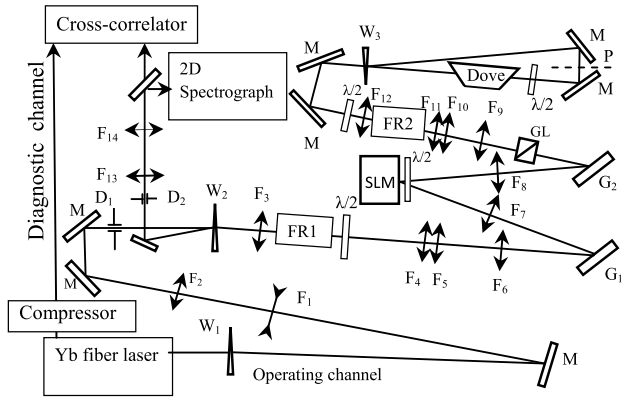

Fig. 3. Schematic diagram of experimental setup: M, mirror; $G_{1,2}$, diffraction gratings; FR1, FR245°, Faraday rotators; SLM, spatial light modulator; GL, Glan prism; W1,2,3, calcite wedges; D1,2, diaphragms; P, plane of image transfer from grating; G_2, F_i (I = 1…14) lenses ($F_1 = -140$ mm, $F_2 = 350$ mm, $F_3 = 400$ mm, $F_4 = 169$ mm, $F_5 = 259$ mm, $F_6 = 369$ mm are spherical; $F_7 = F_8 = 405$ mm are cylindrical; and $F_9 = 368$ mm, $F_{10} = 174$ mm, $F_{11} = 394$ mm, $F_{12} = 414$ mm, $F_{13} = 160$ mm, $F_{14} = 260$ mm are spherical).

to the scanning cross-correlator for measuring temporal and spatial characteristics of the profiled beam.

The fiber laser includes a femtosecond Yb fiber master oscillator operating in the regime of passive mode locking: pulse repetition rate 47.6 MHz, output duration 215 fs, average power 0.45 mW, central wavelength ~1033 nm. Pulses from the master oscillator are forwarded to a 50 m fiber stretcher where they are stretched up to 15 ps and are then amplified in a 1.5 m Yb fiber amplifier pumped by a 400 mW diode pump. An output 50% splitter divides the radiation into two identical channels: diagnostic and operating. Radiation from the operating channel is passed through an acousto-optic modulator for reducing the pulse repetition rate by a factor of 4, 8, 16, 32, and 64. Further, after the second, 80 m stretcher the radiation is amplified in the second Yb fiber amplifier. The maximum peak power of the operating channel is limited by cubic nonlinearity in the second fiber amplifier to 150 W. We obtained pulse duration of output radiation $T = 41$ ps, energy $W = 5.7$ nJ, and spectral width (FWHM) 7.3 nm. With the increase of the output energy $W > 6$ nJ, the spectrum modulation depth increased too and such laser pulses cannot be used for 3D beam shaping.

After a fiber collimator, radiation from the diagnostic channel was passed to the bulk optical compressor having a diffraction grating with 1200 grooves/mm density (Spectrogon, 50 mm × 110 mm). The optical pulse duration measured at the compressor output was 250 fs, which is only slightly higher than the Fourier limit of pulses having spectral width 7.3 nm and central wavelength 1033 nm.

The main and most important part of the experimental setup is the 3D shaper of intensity distribution. Let us consider its operation in more detail. Linear polarization of collimated radiation of the operating channel is attained by means of a 10° calcite wedge W_1. A Galilean-type telescope $F_1 - F_2$ widens the beam and compensates its divergence. Diaphragm D_1 forms the transverse distribution as a Gaussian function with cut wings. The diaphragm plane is translated to the plane of the SLM by means of the lens system $F_3 - F_6$ with magnification 0.8. A Faraday isolator formed by a polarizer of calcite wedge W_2, a 45° Faraday rotator FR1 (with 20 mm aperture of TGG magnetoactive element), and a zero-order half-wave plate extracts counterpropagating radiation from the shaper. Reflecting holographic diffraction gratings G_1 and G_2 (Spectrogon, 50 × 50 mm), cylindrical lenses $F_7 - F_8$, and the SLM form an optical compressor. The radiation passing through the compressor has horizontal polarization (in the plane of the figure). As is seen in Fig. 3, cylindrical lenses $F_7 - F_8$ form a Kepler telescope and an amplitude mask is placed in its focus (SLM, half-wave plate, and Glan prism as a polarizer). In the scheme in Fig. 3, the Glan prism is positioned after diffraction grating G_2 solely for convenience of aligning. The plane of diffraction grating G_1 is translated to the plane of diffraction grating G_2 with magnification 1 in the plane of the figure only. In this case, the beam phase in the orthogonal plane acquires spherical divergence. After direct passage, this phase corresponds to the beam passage of fourfold focal distance of cylindrical lenses (1620 mm in our case). As a result, strong astigmatism arises in the beam that may be corrected by using an additional cylindrical confocal telescope making an angle of 90° with the initial one. If the optical system $F_9 - F_{12}$ transfers the image of the grating G_2 plane to plane P (like in Fig. 3), then the astigmatism acquired after the first passage will be compensated on the backward passage. Note that in the experiment the beam was rotated by 90° either by means of the Dove prism turned by 45° with respect to the beam axis, or using four 45° mirrors folded together forming, in turn, a vertical periscope for rotation and an elevator for returning the beam to the initial height. Direct pass of the 90° rotator and backward pass of the beam to the shaper were accomplished by means of the Faraday isolator: Glan prism, calcite wedge W3, 45° Faraday rotator FR2, and half-wave plate. A half-wave plate placed after the Dove prism makes the polarization of the transmitted radiation vertical. We used pairs of lenses (F4, F5 and F10, F11, see Fig. 3) to minimize the influence of spherical aberration on the laser beam. The used imaging in the optical scheme helps to minimize the influence of beam diffraction and to nullify the impact of possible angular chirp in the translated planes.

Schematic diagrams of the devices used in our research for diagnosing space–time intensity distributions of profiled pulses are presented in Fig. 4. The operation of a cross-correlator [Fig. 4(a)] is based on a noncollinear process of second-harmonic generation occurring during the interaction of profiled and diagnostic pulses in a nonlinear crystal. In our case, the beams intersected in the LBO crystal at an angle of 2°–3° to each other. The first type of interaction (oo-e) was used. As the duration of the pulses in the diagnostic channel was much less than that of the profiled pulses, the intensity distribution of the sum frequency measured by a CCD camera corresponded to the intensity distribution of the profiled pulses. By varying the delay we observed different time sections of the studied pulses. The cross-correlator was described in detail in our earlier work [13].

The use of a 2D spectrograph [Fig. 4(b)] enables measuring 3D spectrum intensity distribution. The image of the profiled beam is transferred to the spectrograph slit. The image of the vertical slit is transferred by means of a lens to the CCD camera through a reflecting holographic diffraction grating with a density of 1200 grooves/mm (Spectrogon, 50 × 110 mm). The beam incident on the slit may be shifted in parallel by means of a micrometer translator, thereby a series of vertical slices spectra are obtained. As was mentioned above, for pulses with significant linear frequency modulation, such measurements correspond to measurements of spatial intensity distribution.

5. SHAPING OF QUASI-CYLINDRICAL BEAMS

To obtain in the experiment pulses with quasi-cylindrical intensity distribution in space there is no need to use the whole

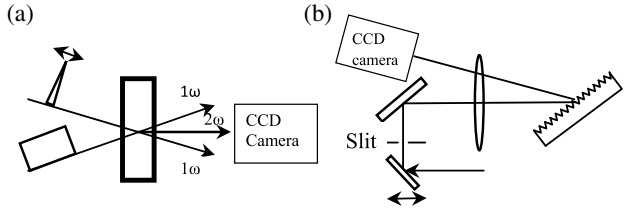

Fig. 4. Schematic diagrams of optical devices used for measuring 3D intensity distribution of profiled pulses: (a) scanning cross-correlator and (b) two-dimensional spectrograph.

3D pulse shaper (Fig. 3). A much simpler scheme may be employed, where the cylindrical lens F_7 is replaced by a spherical one and the SLM is adjusted exactly backward. In this case, the intensity distribution shaper works by a traditional scheme [9] and can control only temporal characteristics of pulses. Note that in our experiment we used the quasi-rectangular amplitude mask Eq. (6) to obtain quasi-cylindrical distributions. Homogeneous round transversal distribution with sharp edges was shaped by means of diaphragm D2 placed in the plane conjugate with the plane of the first diaphragm.

The initial spectrum distribution, i.e., for $M(\omega) = 1$, and with the use of the spectral mask with 7.9 nm transmission band are shown in Fig. 5(a). The measured energy transmittance of the scheme for $M(\omega) = 1$ was about 20%. This value does not take into account energy losses produced by the reference diaphragm D1 (see Fig. 3). Note that in the laser driver for photoinjector PITZ, we placed an analogous optical scheme between forward and backward passes of the main disk amplifier [1] to compensate the energy losses.

The mask in our experiment was not optimal in energy terms. The cross-correlation functions measured for those cases are plotted in Fig. 5(b). The profiled pulse had a rise time of 4 ps, which is in a good agreement with the results of Fig. 2. For $M(\omega) = 1$, the pulse duration at FWHM intensity distribution was 41 ps. To compare the results of the experiment and the theory considered above we performed numerical simulations. The mask Eq. (6) with a full bandwidth of 7.9 nm ($N = 12$) was applied to the initial Gaussian spectrum of 7.3 nm (FWHM) and central wavelength of 1033 nm. Results of the numerical simulation are presented in Figs. 5(a) and 5(b) by dashed lines. As the quasi-rectangular spectral mask forms a quasi-rectangular pulse in the time domain, the temporal distribution repeats the intensity distribution in the spectral region for the experimental conditions. The acquired chirp used to stretch laser pulses has mostly a linear component. So, the described approach to pulse shaping is valid.

The measured spatial transverse intensity distributions at different delays and the reconstructed smoothed quasi-cylindrical structure of the intensity distribution (90 experimental shots) are presented in Fig. 6.

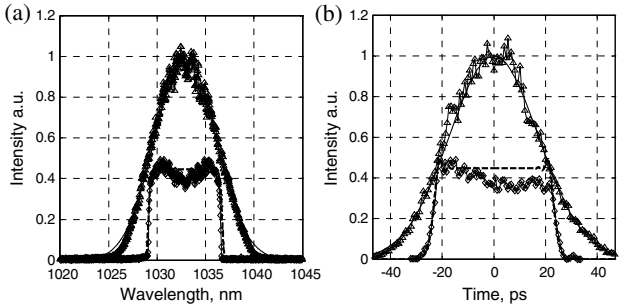

Fig. 5. (a) Experimental data: initial spectrum: triangles, profiled spectrum: rhombs; results of simulation with a mask for Gaussian spectrum distribution: dashed curve, approximation by Gaussian initial spectrum: solid curve. (b) Experimental data: initial cross-correlation function: triangles, profiled function: rhombs; results of simulation with a mask for Gaussian spectrum: dashed curve, Gaussian approximation of initial cross-correlation function: solid curve.

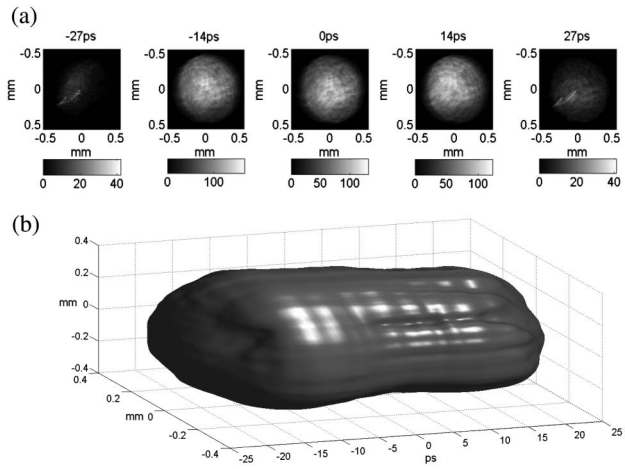

Fig. 6. (a) Measured transverse intensity distributions of quasi-cylindrical pulses; (b) reconstructed 3D distribution.

6. SHAPING OF QUASI-ELLIPSOIDAL BEAMS

In experiments on generating quasi-ellipsoidal beams we used the full scheme of a 3D pulse shaper. A two-dimensional elliptical distribution was used as an amplitude mask. The reflection coefficient of spectral components was equal to unity in the region of the ellipse, and to zero outside it. The beam passed through the amplitude mask twice: on direct and backward passage after a 90° turn in the Dove prism. As a result of double action in orthogonal directions of the same amplitude mask, a beam with quasi-ellipsoidal intensity distribution was formed from the initial beam. The transverse cross sections of the laser beam profiled in this way were squares. The size of the square changed along the propagation axis by ellipsoidal law $a(t) = a_0 \cdot \sqrt{1 - \left(\frac{2 \cdot t}{T_{el}}\right)^2}$, where t is time and T_{el} is the duration of the ellipsoid on the axis.

Quasi-ellipsoidal beams in our experiments were visualized by means of a two-dimensional spectrograph [Fig. 4(b)]. Images of the transverse distribution of the spectral intensity measured with a beam scanning step of 0.15 mm over the spectrograph slit are presented in Fig. 7. Knowing the spectral width of the initial (nonprofiled) pulse of 7.3 nm and pulse duration (FWHM) of 41 ps, one can readily find the wavelength-time scaling rate 41/7.3 ps/nm ≈5.6 ps/nm, assuming linear frequency modulation. To obtain three-dimensional spectrum intensity distributions we recorded a series of frames (50–100 pcs) with 20–50 μm scanning step. The reconstructed intensity distribution for this series is shown in Fig. 8.

It is important to note that, in principle, the proposed method of generating laser pulses with quasi-ellipsoidal

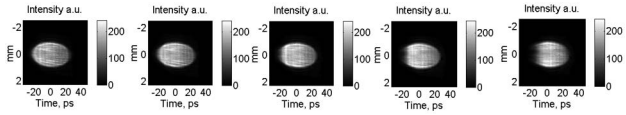

Fig. 7. Different cross sections of the spectrum of quasi-elliptical beam taken with the interval of 0.15 mm.

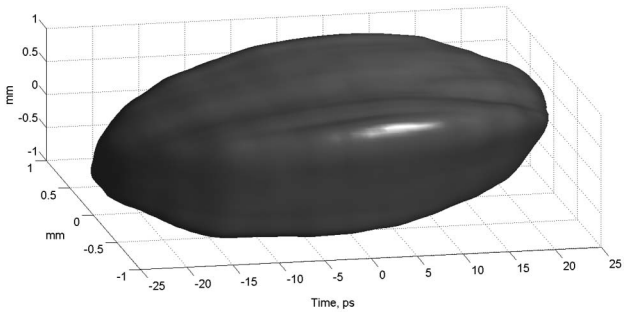

Fig. 8. Quasi-ellipsoidal beam obtained in experiment.

intensity distribution in space does not allow obtaining axially symmetric ellipsoidal distributions. The point is that only 90° rotation of the beam during passage through the 3D pulse shaper is implemented in this method. It is possible to attain an almost ellipsoidal structure by rotating the quasi-ellipsoidal distribution described above by 45° with respect to the propagation axis and then transmitting it through the shaper again.

7. CONCLUSION

In the present work we considered and implemented the approach to space–time profiling of pulses with appreciable linear frequency modulation using spatial light modulators in the scheme of an optical stretcher/compressor with diffraction gratings. Laser beams with quasi-cylindrical and quasi-ellipsoidal intensity distribution were demonstrated in the experiment. Theoretical aspects of the operation of a 3D pulse shaper, its drawbacks and applicability scope were considered.

Funding. Ministry of Education and Science of the Russian Federation (14.Z50.31.0007); Russian Foundation for Basic Research (RFBR) (13-02-91323-SIG_a).

REFERENCES

1. E. I. Gacheva, V. V. Zelenogorskii, A. V. Andrianov, M. Krasilnikov, M. A. Martyanov, S. Yu. Mironov, A. K. Potemkin, E. M. Syresin, F. Stephan, and E. A. Khazanov, "Disk Yb:KGW amplifier of profiled pulses of laser driver for electron photoinjector," Opt. Express **23**, 9627–9639 (2015).
2. A. K. Potemkin, E. I. Gacheva, V. V. Zelenogorskii, E. V. Katin, I. E. Kozhevatov, V. V. Lozhkarev, G. A. Luchinin, D. E. Silin, E. A. Khazanov, D. V. Trubnikov, G. D. Shirkov, M. Kuriki, and J. Urakava, "Laser driver for a photocathode of an electron linear accelerator," Quantum Electron. **40**, 1123–1130 (2010).
3. XFEL, "Interim report of the scientific and technical issues (XFEL-STI) working group on a European XFEL facility in Hamburg," Interim Report, 2005.
4. M. Krasilnikov, F. Stephan, G. Asova, H.-J. Grabosch, M. Groß, L. Hakobyan, I. Isaev, Y. Ivanisenko, L. Jachmann, M. Khojoyan, G. Klemz, W. Köhler, M. Mahgoub, D. Malyutin, M. Nozdrin, A. Oppelt, M. Otevrel, B. Petrosyan, S. Rimjaem, A. Shapovalov, G. Vashchenko, S. Weidinger, R. Wenndorff, K. Flöttmann, M. Hoffmann, S. Lederer, H. Schlarb, S. Schreiber, I. Templin, I. Will, V. Paramonov, and D. Richter, "Experimentally minimized beam emittance from an L-band photoinjector," Phys. Rev. Spec. Top. Accel. Beams **15**, 100701 (2012).
5. I. Will and G. Klemz, "Generation of flat-top picosecond pulses by coherent pulse stacking in a multicrystal birefringent filter," Opt. Express **16**, 14922–14937 (2008).
6. F. Stephan and M. Krasilnikov, "High brightness photo injectors for brilliant light sources," in *Synchrotron Light Sources and Free-Electron Lasers* (Springer, 2014), pp. 1–38.
7. I. M. Kapchinskij and V. V. Vladimirskij, "Limitations of proton beam current in a strong focusing linear accelerator associated with the beam space charge," in *Proceedings of the International Conference on High-Energy Accelerators and Instrumentation* (CERN, 1959), pp. 274–288.
8. Y. Li, S. Chemerisov, and J. Lewellen, "Laser pulse shaping for generating uniform three dimensional ellipsoidal electron beams," Phys. Rev. Spec. Top. Accel. Beams **12**, 020702 (2009).
9. M. Wefers and K. Nelson, "Generation of high-fidelity programmable ultrafast optical waveforms," Opt. Lett. **20**, 1047–1049 (1995).
10. S. A. Akhmanov, V. A. Vysloukh, and A. S. Chirkin, *Optics of Femtosecond Laser Pulses* (Nauka, 1988), Chap. 1, p. 43.
11. A. K. Potemkin, E. V. Katin, A. V. Kirsanov, G. A. Luchinin, A. N. Mal'shakov, M. A. Mart'yanov, A. Z. Matveev, O. V. Palashov, E. A. Khazanov, and A. A. Shaikin, "Compact neodymium phosphate glass laser emitting 100-J, 100-GW pulses for pumping a parametric amplifier of chirped pulses," Quantum Electron. **35**, 302–310 (2005).
12. http://www.pishaper.com/public.php.
13. V. V. Zelenogorskii, A. V. Andrianov, E. I. Gacheva, G. V. Gelikonov, M. Krasilnikov, M. A. Mart'yanov, S. Yu. Mironov, A. K. Potemkin, E. M. Syresin, F. Stephan, and E. A. Khazanov, "Scanning cross-correlator for monitoring uniform 3D ellipsoidal laser beams," Quantum Electron. **44**, 76–82 (2014).